JACS
JOURNAL OF THE AMERICAN CHEMICAL SOCIETY

Article

Trap-Enabled Long-Distance Carrier Transport in Perovskite Quantum Wells

Chunyi Zhao, Wenming Tian, Qi Sun, Zixi Yin, Jing Leng, Shiping Wang, Junxue Liu, Kaifeng Wu, and Shengye Jin

J. Am. Chem. Soc., **Just Accepted Manuscript** • DOI: 10.1021/jacs.0c06572 • Publication Date (Web): 05 Aug 2020

Just Accepted

is published by the American Chemical Society. 1155 Sixteenth Street N.W., Washington, DC 20036

Trap-Enabled Long-Distance Carrier Transport in Perovskite Quantum Wells

Chunyi Zhao[1, 2], Wenming Tian[1,], Qi Sun[1, 2], Zixi Yin[1, 2], Jing Leng[1], Shiping Wang[1, 2], Junxue Liu[1], Kaifeng Wu[1,*], Shengye Jin[1,*]*

[1]State key laboratory of molecular reaction dynamics and the dynamic research center for energy and environmental materials, Dalian Institute of Chemical Physics, Chinese Academy of Sciences, Dalian 116023, China

[2]University of Chinese Academy of Sciences, Beijing 100049, China

[*] Corresponding: sjin@dicp.ac.cn; kwu@dicp.ac.cn; tianwm@dicp.ac.cn.

Abstract： Layered two-dimensional (2D) hybrid perovskites are naturally-formed multiple quantum well (QW) materials with promising applications in quantum and optoelectronic devices. In principle, the transport of excitons in 2D perovskites is limited by their short lifetime and small mobility to a distance within a few hundreds of nanometers. Herein, we report an observation of long-distance carrier transport over 2 to 5 micrometers in 2D perovskites with various well thicknesses. Such a long transport distance is enabled by trap-induced exciton dissociation into long-lived and nonluminescent electron-hole separated state, followed by a trap-mediated charge transport process. This unique property makes 2D perovskites comparable with 3D perovskites and other traditional semiconductor QWs in terms of carrier transport property and highlights their potential application as an efficient energy/charge-delivery material.

INTRODUCTION

Two-dimensional (2D) Ruddlesden-Popper layered perovskites are emerging as a promising material for optoelectronic and quantum devices.[1-5] Given a general formula of $(RNH_3)_2(B)_{n-1}Pb_nX_{3n+1}$ (R is an alkyl or aromatic group, B is organic cation and X is halide), layered 2D perovskites are multiple quantum well (QW) materials. They have attracted great attention because of many unique features such as flexible structures, large exciton binding energy, readily tunable bandgap (thickness of QW) and prominently improved moisture resistance.[6-8] These properties have led to many demonstrations of 2D (or quasi-2D) perovskite devices with improvement in stability and optoelectronic performance.[9-15] However, 2D perovskite is also believed to possess a relatively poor carrier transport property, particular when compared to its 3D counterpart and other classical semiconductor QWs such as $GaAs/Al_xGa_{1-x}As$. For 3D perovskites such as $CH_3NH_3PbX_3$, a key enabling their remarkable success in optoelectronic application is the super long carrier diffusion length up to a few micrometers or even longer[16-19]. $GaAs/Al_xGa_{1-x}As$ QW also exhibits long carrier transport on micrometer scale because of its super high charge mobility.[20-22] In sharp contrast, excitons in 2D perovskite are stable at room temperature due to their large binding energy (~100 to 400 meV),[23-25] and their transport is confined in the QW plane with a diffusion distance limited by a short exciton lifetime and small mobility. With a typical lifetime value of a few to tens of ns, the diffusion length of band-edge excitons in 2D perovskites with $n \leqslant 4$ was found to be about < 100 to 500 nm,[26, 27] more than an order of magnitude shorter than that in 3D perovskite crystals.

Therefore, in terms of the exciton/carrier transport property as reported in previous works, 2D perovskites supposedly might not be able to compete with 3D perovskites and other traditional semiconductor QWs.

Herein, we report a surprising observation of long-distance carrier transport beyond the limit of exciton in pure-phase layered 2D perovskites. We find that their carrier diffusion distance can be surprisingly as long as 2 to 5 μm, which is on the same order of 3D perovskites and other traditional semiconductor QWs.

RESULTS AND DISCUSSION

Our measurement was performed on exfoliated $(PEA)_2(MA)_{n-1}Pb_nI_{3n+1}$ (PEA = $C_6H_5C_2H_4NH_3^+$, MA = $CH_3NH_3^+$) perovskites (n = 2, 3 and 4) single crystals by using time-resolved photoluminescence (PL) imaging microscope with a sub-micrometer spatial resolution. Unlike the traditional confocal PL microscope, our setup is capable of scanning the PL collection pathway across the sample by using a pair of galvano-mirror and meanwhile fixing the excitation laser at a specific position (see setup in Figure S1 in the supporting information (SI)). The same setup has been successfully utilized to directly visualize carrier emission and transport in nanostructured 3D perovskites.[28-30] In this work, however, we find that carriers in 2D perovskites travel in a nonluminescent (dark) state, making the transport process "unseen" by only collecting exciton emission. Fortunately, the presence of low-energy (LE) emission sites (in addition to bandgap emission) specifically locating at

exfoliated crystals edges,[4, 26, 31-33] provides a unique spectroscopic handle for us to observe such "dark" carrier transport. Specifically, we find that these LE sites can collect the "dark" carriers diffusing from an excitation spot a few micrometers away and then turn them into an emissive state, whose LE PL kinetics can thus reflect the "dark" carrier transport process. We propose that the long-distance carrier transport in 2D perovskites is enabled by trap-induced exciton dissociation into a long-lived (several hundreds of ns) and nonluminescent electron-hole separated state, followed by a trap-mediated charge transport process.

We first carried out the static PL measurements to show the presence of LE emission sites in 2D perovskite crystals (Figure 1). The schematic crystal structure of $(PEA)_2(MA)_{n-1}Pb_nI_{3n+1}$ is shown in Figure 1a. The X-ray diffraction (XRD) patterns and the scanning electron microscopy images of these 2D perovskites are shown in Figure S2 and S3. Figure 1b shows the absorption spectra of bulk $(PEA)_2(MA)_{n-1}Pb_nI_{3n+1}$ perovskites with n = 2, 3 and 4. The increase in bandgap (BG) energy from ~1.88 eV (660 nm) to ~2.12 eV (585 nm) from n = 4 to 2 is due to the quantum and dielectric confinement effect.[7, 34] For microscopic PL spectroscopy and imaging measurements, mechanically exfoliated 2D crystals were prepared and transferred on glass cover slips. The presence of LE emission can be confirmed in microscopic emission spectra from some selected exfoliated crystals, which show both BG emission peaks and LE emission from 730 to 770 nm (Figure 1c). The spatial location of LE sites can be identified in the microscopic PL images on an exfoliated crystal (n = 3) collected in both BG and LE emission channels (Figure 1d). In this

image, the crystal was excited homogeneously by a de-colliminated laser and the BG and LE emission signals are merged in one image for a better comparison. The original images from BG and LE emission channels and the image processing procedure are shown in Figure S4. The PL image shows a uniform distribution of BG emission on the crystal, with a few isolated LE emission sites particularly located at the crystal edges. Similar PL images were also obtained for n = 2 and n = 4 exfoliated crystals (Figure S5).

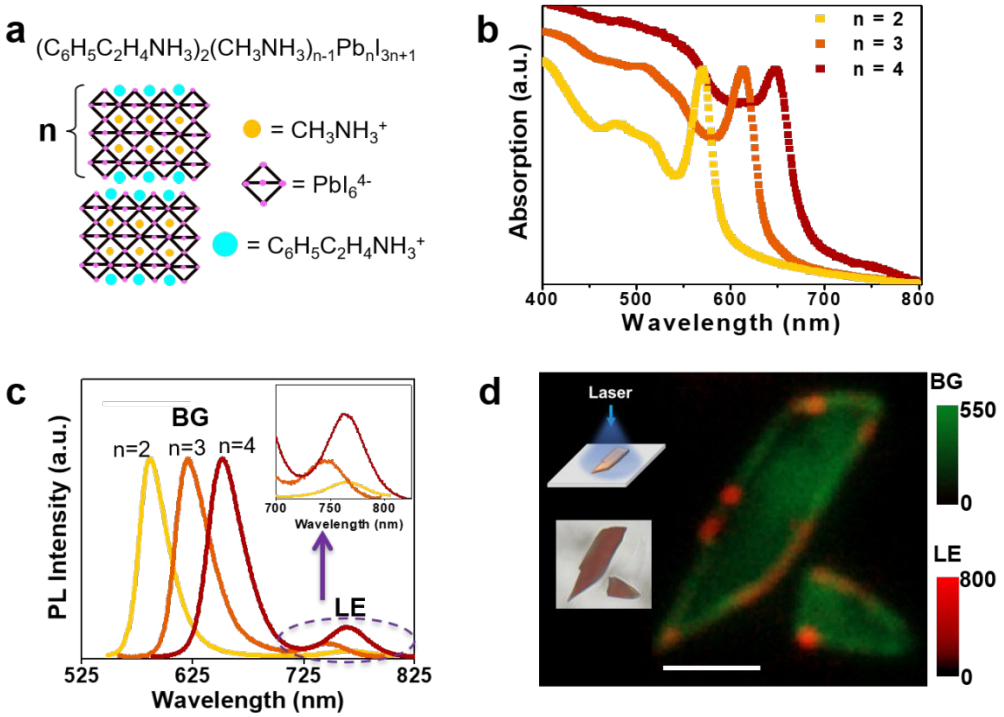

Figure 1. Spectroscopic and microscopic PL characterizations of 2D perovskite crystals. (a) Schematic of the crystal structure of $(PEA)_2(MA)_{n-1}Pb_nI_{3n+1}$ 2D perovskite. (b) UV-vis absorption spectra of pristine 2D perovskites with n = 2, 3, 4. (c) Microscopic PL spectra of exfoliated 2D crystals with n = 2, 3 and 4, showing both bandgap (BG) exciton emission and a low energy (LE) emission from 730 to 770 nm. (d) Microscopic PL intensity image of an exfoliated crystal (n = 3) comprised of both BG (green) and LE (red) emissions, showing a few LE emission sites at the crystal edge. The insets show the optical image of the crystal and the homogeneous

excitation configuration. The scale bar is 5 μm.

This observation of LE emission at crystal edges agrees with previous reports.[4, 26, 31-33] The LE sites are likely generated during initial fabrication or in the exfoliation process. They were previously named as an "edge state", which can collect the BG excitons and facilitate exciton dissociation into long-lived free charges.[4, 26] Our and other's recent works further demonstrated that the LE sites were actually local structural impurity domains formed by the stochastically loss of spacer ligands (thus the quantum confinement effect) at crystal edges, and they therefore can exhibit a photophysical property similar as 3D perovskites.[31, 32]

For the 2D crystals with LE emission sites, a very interesting phenomenon is observed in their PL images when we used a focused laser beam to excite the crystal (Figure 2a and Figure S6). The PL images are obtained by scanning the PL collection path (both BG and LE emission channels) over the crystal, with the excitation spot (~1 μm diameter) fixed at the central area of the crystal where there is no LE site. Even though the excitation spot is a few micrometers away, appreciable LE emission is still observed from LE sites at crystal edge (Figure 2a and Figure S6). A more surprising aspect in these PL images (Figure 2a and Figure S6) is that the BG exciton emission is confined in the excitation spot and no PL appears between the excitation spot and LE sites. This phenomenon can be better visualized in a set of PL images collected at various delay times after excitation (Figure 2b and Figure S7, please also see the Movie in online SI). The BG emission at the excitation spot decays quickly

within the first tens of ns after excitation, which is consistent with the short exciton lifetime. After the BG emission disappears, PL from LE sites at the crystal edge progressively forms on the time scale > 100 ns. These images are in sharp contrast to the case of 3D perovskites, where the carriers are luminescent when they diffuse away from the excitation spot (Figure S9), indicating that the carrier transport mechanisms in 2D and 3D perovskites are very different. Therefore, the PL images of 2D perovskites imply that some carriers can travel in a nonluminescent state, rather than in the bright excitonic state. This result also confirms that the diffusion length of BG exciton in 2D crystal should be much smaller than our microscopic spatial resolution, in agreement with the reported exciton diffusion length within a few hundreds of nanometers.[27]

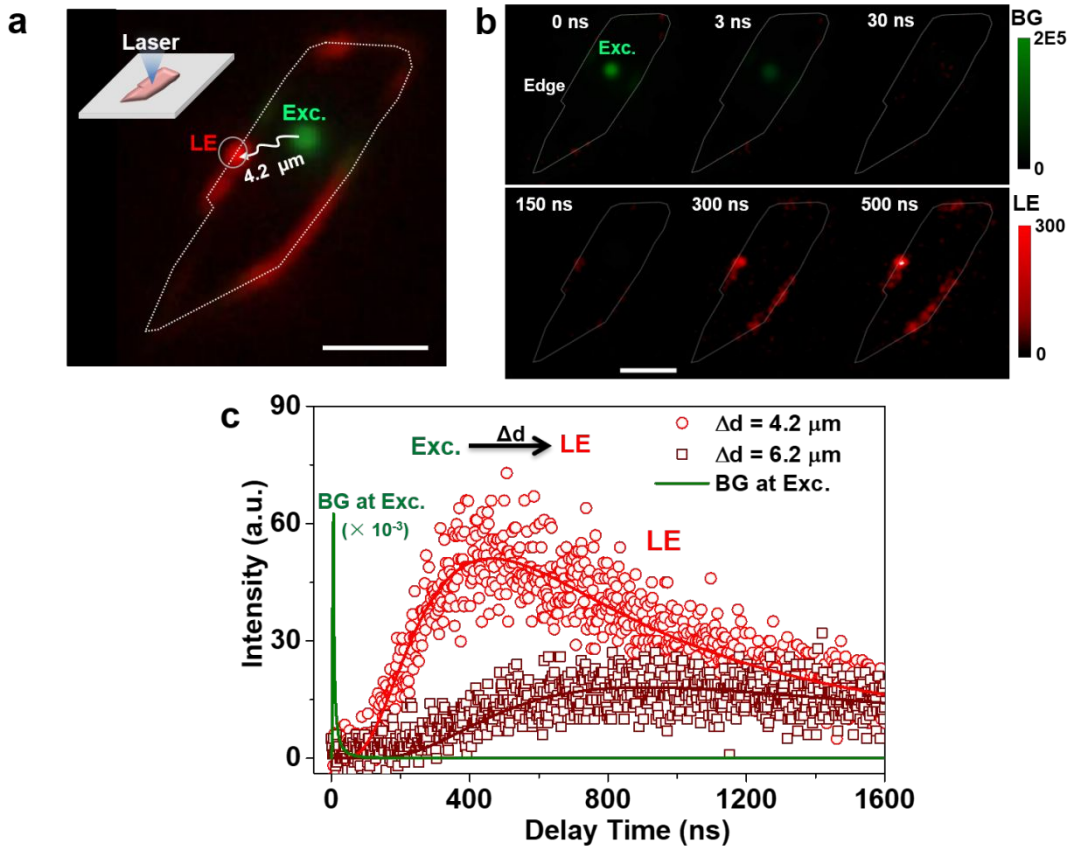

Figure 2. Long-distance carrier transport in an exfoliated 2D perovskite crystal (n = 3) revealed by time-resolved PL images and kinetics. (a) Microscopic PL intensity image of the same crystal as in Figure 1d under a focused excitation (Exc.) laser beam (~ 1 μm diameter) with a few micrometers of distance to LE sites. This image shows BG PL at the excitation spot and LE PL at the crystal edge but with no PL appearance in between, implying a carrier transport in a nonluminescent state until reaching the LE sites, where the carriers return to a luminescent state with LE PL. The inset illustrates the excitation configuration. Scale bar is 5 μm. (b) A set of PL intensity images at different delay times after excitation, showing the evolution of BG and LE PL signals. Scale bar is 5 μm. (c) BG and LE TRPL kinetics collected at the excitation spot and a selected LE site with excitation-to-LE distances (Δd) of 4.2 μm and 6.2 μm. The solid lines are the fits of the LE TRPL according to the simulation model described in SI.

We also extracted the time-resolved PL (TRPL) kinetics at a selected LE site and at the excitation spot within a time window of 2000 ns (Figure 2c). For an

excitation-to-LE distance (Δd) of ~4.2 μm, the kinetics of LE PL, in contrast to the fast decay of BG PL, displays a slow rising component in the first 400 ns followed by a slow decay process. In addition, if the excitation spot was moved further away (Δd = 6.2 μm) from the monitored LE site (Figure 2c), the LE PL kinetics becomes slower in the rising component with a smaller PL intensity. These kinetics reflect the carrier transport process from the excitation spot to the LE site, where the carriers accumulate and relax by emitting LE PL. This distance-dependent kinetics should also rule out the possibility of direct excitation of LE site by BG emission photons or a photon recycling process, in which case the PL kinetics should not exhibit such a prominent distance-dependence (see SI for detail discussions).

The above result uncovers intriguing carrier transport features in 2D perovskite crystal, that are summarized as: i) a portion of photoinduced BG carriers can diffuse over a long distance in a nonluminescent state, rather than in a bright excitonic state; ii) the "dark" carriers have a long lifetime to enable a long-range transport over a few micrometers; iii) the "dark" carriers can be collected at the LE site and return to a luminescent state. We confirm that these features are common in 2D perovskites by also observing the similar time-resolved PL images and kinetics for n = 2 and 4 crystals (Figure S7 and S10).

To understand the carrier transport mechanism in 2D perovskites, we first need to elucidate how the bright BG excitons are transformed into a long-lived "dark" state. Recent reports revealed that both 3D and 2D hybrid perovskites exhibit a slightly indirect band character at conduction band minimum due to a combination of

inversion symmetry breaking and spin-orbit coupling effects (Rashba splitting)[35]. At the indirect band, carrier recombination is suppressed because of the shift in *k*-space between the conduction band minimum and valance band maximum. However, the energy difference between direct and indirect bands is only 20 ~ 75 meV,[35-37] which should not strongly modulate carrier emission and transport at room temperature. Similarly, the possibility of exciton transport in a dark triplet state can also be excluded because the exchange splitting is only a few meV.[38]

Another possibility is trap-induced exciton dissociation into a long-lived and nonluminescent electron-hole separated state. Such exciton dissociation has been observed in CdS or PbS quantum dots, where the separated electron and hole can show a lifetime up to hundreds of nanoseconds or even microsecond.[39-43] Previous theoretical calculations also indicate that in $CH_3NH_3PbI_3$ 3D perovskites, the iodine interstitial defect is a hole trap state close to valance band (VB), which can prolong the lifetime of free charges and facilitate charge transport through an effective trapping and reverse (detrapping) process.[44] To examine this probability in 2D perovskites, we performed an excitation-intensity-dependent TRPL measurement on BG excitons (Figure 3a for n = 3 and Figure S11 for n = 2 and n = 4 perovskites). At the lowest examined excitation intensity, the exciton TRPL kinetics is dominated (with a ~90% amplitude) by a fast decay component close to our instrument response function (IRF of 130 ps), followed by a slow component on tens of ns time scale, and the amplitude of fast component decreases as the excitation intensity increases. The fast decay component was also observed in other 2D perovskites and can be explained

by the existence of trap states,[45] which cause a fast initial drop of PL intensity through electron or hole trapping. The amplitude of fast decay component depends on the ratio of trap state density (N_{trap}) in relative to the density of exciton ($N_{exciton}$). When $N_{trap} >$ or $\approx$ $N_{exciton}$ (at low excitation intensity), the fast trapping process can dominate the TRPL decay; when $N_{exciton} >> N_{trap}$ (at high excitation intensity), the trap states can be fully filled and their influence to TRPL becomes negligible. There is no direct evidence to identify the trap state as a hole or electron trap; however, considering that perovskite layer in 2D crystal has the same structure as $CH_3NH_3PbI_3$ 3D perovskite, we speculate that the trap state in 2D perovskites could also be a hole trap created by iodine interstitial defect as in previous theoretical calculation.[44]

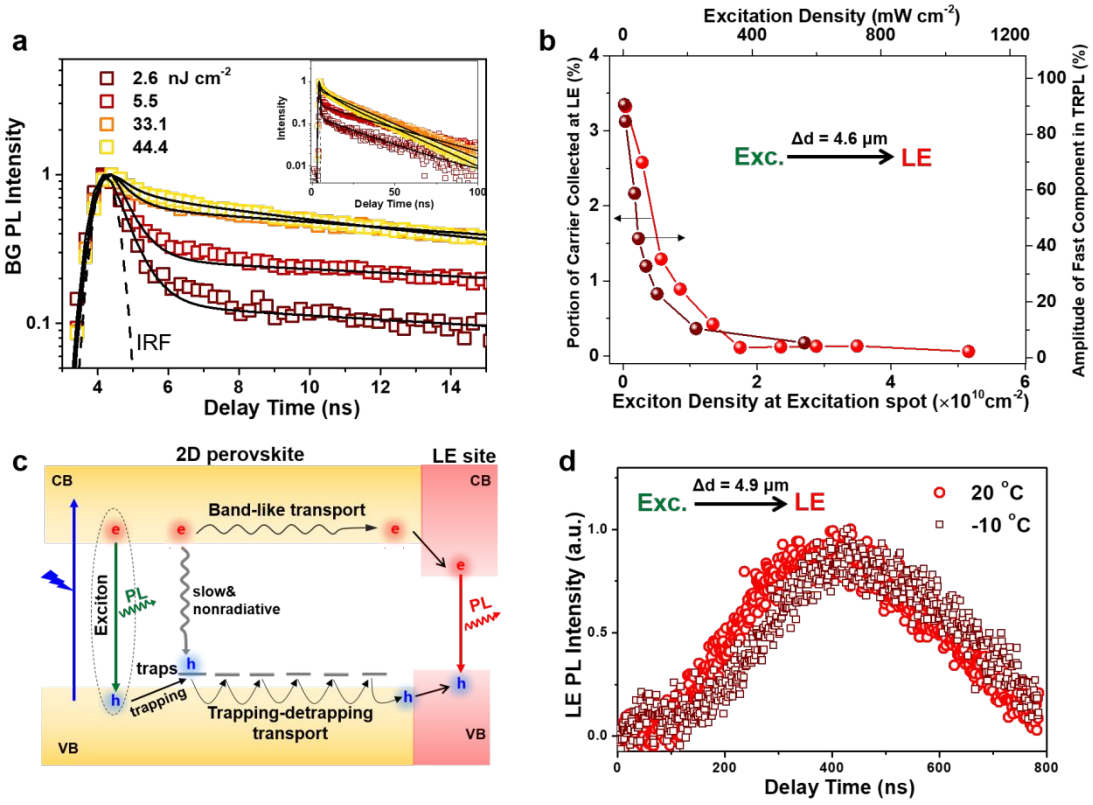

Figure 3. Carrier transport mechanism in layered 2D perovskites. (a) TRPL decays of BG exciton within a time window of 15 ns under different excitation intensities in a typical n = 3 perovskite crystal, showing the change of fast component amplitude with excitation intensity. The inset shows the TRPL in a larger time window. Black lines are fits of the decay curves with a multi-exponential function. (b) Portion of carriers collected at a LE site in relative to the exciton density generated at excitation spot in a typical n = 3 perovskite crystal. The excitation-to-LE distance (Δd) is 4.6 μm. The exciton density generated at the excitation spot is varied by changing the excitation intensity at 450 nm. Also compared in the panel is a plot of fast component amplitude in BG TRPL as a function of excitation intensity at the excitation spot. (c) Schematic of a trap-mediated transport mechanism in 2D layered perovskites. (d) Temperature-dependent LE PL kinetics collected at a LE site with Δd = 4.9 μm in a typical n = 3 perovskite crystal.

If the carriers diffusing to LE sites are indeed separated electrons and holes after trap-induced exciton dissociation, the proportion of carriers collected at LE site to the total number of excitons generated at the excitation spot should also exhibit excitation-intensity dependence. For a representative 2D crystal with n = 3, Figure 3b shows the relative carrier population collected at a LE site as a function of exciton density generated at excitation spot (varied by changing excitation intensity). The corresponding PL spectra at various exciton densities are shown in Figure S12. For a travel distance of 4.6 μm, a larger portion of carriers is collected at the LE site when the exciton density generated at the excitation spot is smaller (corresponding to lower excitation intensity) (see SI for the estimation of carrier population). This trend is overall consistent with the amplitude of fast component in the intensity-dependent TRPL traces of BG exciton (Figure 3b). Similar results were also found for n = 2 and n = 4 crystals (Figure S13). The slight inconsistency between the two plots is likely caused by the TRPL fitting errors and the errors in the estimation of carrier portion collected at the LE site. This result implies that the "dark" carriers in the long-range transport are very likely the long-lived and nonluminescent separated charges generated by trap-induced exciton dissociation.

The above results lead us to propose a long-range carrier transport mechanism in 2D perovskite QWs with n = 2 ~ 4 (Figure 3c). Upon excitation, a portion of excitons undergoes a fast dissociation process, generating a charge-separated state with hole at a trap state and electron at conduction band (CB). The recombination of electron at CB with the trapped hole is slow (on hundreds of ns time scale) and nonradiative, thus

enabling a long-range transport with little PL in the pathway. Once they reach a LE site, the electron and hole can be collected and turn into a luminescent state with LE PL. The transport of electron is band-like, while the hole transport is mediated by the trap state, through a consecutive trapping-detrapping process. The latter should be a thermally activated process. Indeed, the LE TRPL trace, collected from a LE site with a distance of 4.9 μm to the excitation spot in a representative 2D crystal with n = 3 (Figure 3d), shows a slower rising kinetics as temperature changes from 20 to -10 °C, indicating a slower carrier transport velocity at a lower temperature. Other n-value 2D crystals also exhibit similar temperature dependence (Figure S14).

In order to quantify the carrier transport parameters, we established a model (see detail in SI) to simulate carrier transport process in 2D perovskite crystals. A global fit of LE PL kinetics with different transport distances by the simulation model can generate the carrier diffusivity (D), carrier lifetime (τ) in charge separated state and then the carrier diffusion length (L_D). For a series of 2D perovskites crystals with different n values, the experimental data are found to be well described by the model (Figure 2c and Figure S15, S16, S17), and the fitting parameters are summarized in Table S1 and S2. Because the LE PL is a result of electron-hole recombination at LE site, the measured diffusivity contains contributions from both hole and electron transports. However, because the trap-mediated hole transport should be much slower than the band transport of free electron, the measured D value is limited by the slow hole transport process. The diffusivity of 2D perovskites are found to be 0.081 ± 0.031 (n = 2), 0.115 ± 0.03 (n = 3) and 0.405 ± 0.2 cm^2/s (n = 4) (Figure 4a). The

carrier lifetimes at electron-hole separated state are found to be 147 ns to 1597 ns (Table S2); using $L_D = (D\tau)^{1/2}$, we calculated the theoretical L_D to be 2 ~ 5 μm in 2D perovskites with n = 2 ~ 4. (Figure 4a), which is a value comparable with those in 3D perovskite single-crystals and also in other classical semiconductor QWs.[17, 18, 21, 28]

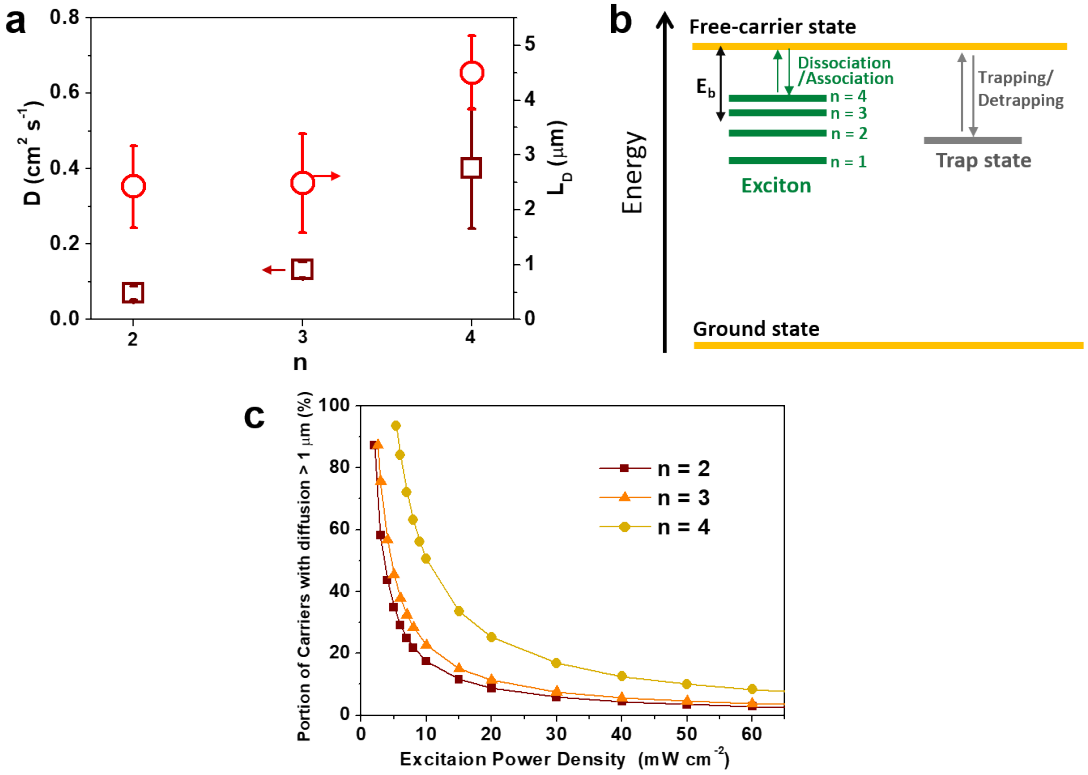

Figure 4. Carrier transport parameters in 2D layered perovskites with n = 2, 3 and 4. (a) Carrier diffusivity (D) and diffusion length (L_D) of 2D layered perovskites with n = 2, 3 and 4. L_D is calculated via equation $L_D = (D\tau)^{1/2}$, where τ is carrier lifetime in an electron-hole separated state generated by trap-induced exciton dissociation. (b) Energy diagram showing the relative energetic positions of exciton with n = 1 ~ 4, free-carrier state and the trap state mediating the charge transport. The difference between the free-carrier state and exciton is exciton binding energy (E_b). (c) Calculated portion of carriers (in relative to the total photogenerated excitons) that can diffuse ≥ 1 μm at different excitation power density for n = 2, 3 and 4 2D perovskites.

Note that, however, such long-distance carrier transport is not observed in n = 1 2D perovskites (Figure S18). On the basis of a homogeneous illumination experiment (Figure S19 and S20), we speculate that the carriers in n = 1 crystal may still follow the same trap-mediated transport mechanism, but with a diffusion length shorter than our instrument spatial resolution (see SI for discussions). By simulating the LE PL kinetics, we determined D = 0.075 cm^2 s^{-1}, τ = 30 ns (separated charge lifetime) (Figure S21) and L_D = 473 nm in a typical n = 1 2D perovskite crystal. Though the L_D is shorter than n = 2 ~ 4 perovskites, it is still much longer than the exciton diffusion length in n = 1 2D perovskite.[27]

The layer thickness dependent carrier diffusivity is consistent with our trap-mediated diffusion model. In this model, the inter-conversion between the BG exciton states and trap states are mediated by the high-energy BG free-carrier states (Figure 4b). Because of an increasing exciton binding energy with decreasing layer thickness, thermally-activated exciton dissociation becomes slower, which eventually limits the carrier diffusivity. In particular, for the n = 1 perovskite, the exciton binding energy might be so strong that it exceeds that the energy difference between the free-carrier and trap states (*i.e.*, trap depth). As a result, exciton states dominate over trap states at equilibrium, leading to inefficient carrier transport, which is in line with our experimental observation.

Because the hole transport is mediated by the trap state, the measured transport parameters are particularly associated with a specific portion of carriers, whose amount is limited by the density of hole traps (N_{trap}). The exciton TRPL result in

Figure 3a illustrates that the trapping process is much faster than the exciton lifetime (10s of ns), suggesting that the majority of excitons can dissociated into trapped holes and free electrons when $N_{trap} \approx N_{exciton}$. As the excitation intensity increases, $N_{exciton}$ will become larger than N_{trap}. The portion of carriers that can perform a long-range diffusion depends on the ratio of $N_{trap}/N_{exciton}$. Combining the diffusivity values, we calculated portion of carriers with a diffusion distance $\geq$ 1 μm in 2D perovskites at different excitation (at 405 nm) power density (Figure 4c, and see SI for the detail of calculation). This result indicates the efficiency of trap-mediated carrier transport in the 2D perovskites for long-distance carrier and energy delivery.

CONCLUSION

In summary, we report an unprecedented observation of long-distance carrier transport beyond the limit of exciton in pure-phase layered $(PEA)_2(MA)_{n-1}Pb_nI_{3n+1}$ 2D perovskites. Their carrier diffusion distance for n = 2 to 4 2D perovskites can be as long as 2 ~ 5 micrometers, which is on the same order of 3D perovskites and other traditional semiconductor QWs. We propose that the long-distance carrier transport in 2D perovskites is enabled by trap-induced exciton dissociation into a long-lived (hundreds of ns) and nonluminescent electron-hole separated state, followed by a trap-mediated charge transport process. We believe this trap-mediated long-distance carrier transport should also occur in other layered 2D perovskites with different chemical compositions. This unique property makes organic-inorganic hybrid 2D perovskites an ideal candidate for high-efficiency optoelectronic and other devices

whose performance relies on a long-range carrier or energy flow.

ASSOCIATED CONTENT

Supporting Information.

Synthesis of samples; experimental setup; XRD, SEM, UV-vis absorption and PL measurements; simulation of carrier diffusion; additional results of measurements. This material is available free of charge via the Internet at http://pubs.acs.org."

AUTHOR INFORMATION

Corresponding Author

sjin@dicp.ac.cn;

kwu@dicp.ac.cn;

tianwm@dicp.ac.cn.

Notes

The authors declare no competing financial interest.

ACKNOWLEDGMENTS

S. Jin thanks the financial support from NSFC (21725305), the MOST (2018YFA0208704，2016YFA0200602) and the Strategic Priority Research Program of CAS (XDB17000000); W. Tian thanks the financial support from NSFC (21703241) and Youth Innovation Promotion Association CAS (2019188).

REFERENCES

(1) Tsai, H.; Asadpour, R.; Blancon, J. C.; Stoumpos, C. C.; Even, J.; Ajayan, P. M.; Kanatzidis, M. G.; Alam, M. A.; Mohite, A. D.; Nie, W. Design principles for electronic charge transport in solution-processed vertically stacked 2D perovskite quantum wells. *Nat. Commun.* **2018**, *9*, 2130.

(2) Tsai, H.; Nie, W.; Blancon, J.-C.; Stoumpos, C. C.; Soe, C. M. M.; Yoo, J.; Crochet, J.; Tretiak, S.; Even, J.; Sadhanala, A.; Azzellino, G.; Brenes, R.; Ajayan, P. M.; Bulovic, V.; Stranks, S. D.; Friend, R. H.; Kanatzidis, M. G.; Mohite, A. D. Stable light-emitting diodes using phase-pure Ruddlesden-Popper layered perovskites. *Adv. Mater.* **2018**, *30*, 1704217.

(3) Leng, K.; Abdelwahab, I.; Verzhbitskiy, I.; Telychko, M.; Chu, L.; Fu, W.; Chi, X.; Guo, N.; Chen, Z.; Chen, Z.; Zhang, C.; Xu, Q.-H.; Lu, J.; Chhowalla, M.; Eda, G.; Loh, K. P. Molecularly thin two-dimensional hybrid perovskites with tunable optoelectronic properties due to reversible surface relaxation. *Nat. Mater.* **2018**, *17*, 908-914.

(4) Feng, J.; Gong, C.; Gao, H.; Wen, W.; Gong, Y.; Jiang, X.; Zhang, B.; Wu, Y.; Wu, Y.; Fu, H.; Jiang, L.; Zhang, X. Single-crystalline layered metal-halide perovskite nanowires for ultrasensitive photodetectors. *Nat. Electron.* **2018**, *1* , 404-410.

(5) Gong, X.; Voznyy, O.; Jain, A.; Liu, W.; Sabatini, R.; Piontkowski, Z.; Walters, G.; Bappi, G.; Nokhrin, S.; Bushuyev, O.; Yuan, M.; Comin, R.; McCamant, D.; Kelley, S. O.; Sargent, E. H. Electron-phonon interaction in efficient perovskite blue emitters. *Nat. Mater.* **2018**, *17*, 550-556.

(6) Quan, L.; Yuan, M.; Comin, R.; Voznyy, O.; Beauregard, E. M.; Hoogland, S.; Buin, A.; Kirmani, A. R.; Zhao, K.; Amassian, A.; Kim, D. H.; Sargent, E. H. Ligand-stabilized reduced-dimensionality perovskites. *J. Am. Chem. Soc.* **2016**, *138*, 2649-2655.

(7) Cao, D.; Stoumpos, C. C.; Farha, O. K.; Hupp, J. T.; Kanatzidis, M. G. 2D homologous perovskites as light-absorbing materials for solar cell applications. *J. Am. Chem. Soc.* **2015**, *137*,

7843-7850.

(8) Quintero-Bermudez, R.; Gold-Parker, A.; Proppe, A. H.; Munir, R.; Yang, Z.; Kelley, S. O.; Amassian, A.; Toney, M. F.; Sargent, E. H. Compositional and orientational control in metal halide perovskites of reduced dimensionality. *Nat. Mater.* **2018**, *17*, 900-907.

(9) Tsai, H.; Nie, W.; Blancon, J. C.; Stoumpos, C. C.; Asadpour, R.; Harutyunyan, B.; Neukirch, A. J.; Verduzco, R.; Crochet, J. J.; Tretiak, S.; Pedesseau, L.; Even, J.; Alam, M. A.; Gupta, G.; Lou, J.; Ajayan, P. M.; Bedzyk, M. J.; Kanatzidis, M. G.; Mohite, A. D. High-efficiency two-dimensional Ruddlesden-Popper perovskite solar cells. *Nature* **2016**, *536*, 312-316.

(10) Wang, N.; Cheng, L.; Ge, R.; Zhang, S.; Miao, Y.; Zou, W.; Yi, C.; Sun, Y.; Cao, Y.; Yang, R.; Wei, Y.; Guo, Q.; Ke, Y.; Yu, M.; Jin, Y.; Liu, Y.; Ding, Q.; Di, D.; Yang, L.; Xing, G.; Tian, H.; Jin, C.; Gao, F.; Friend, R. H.; Wang, J.; Huang, W. Perovskite light-emitting diodes based on solution-processed self-organized multiple quantum wells. *Nat. Photonics* **2016**, *10*, 699-704.

(11) Yuan, M.; Quan, L.; Comin, R.; Walters, G.; Sabatini, R.; Voznyy, O.; Hoogland, S.; Zhao, Y.; Beauregard, E. M.; Kanjanaboos, P.; Lu, Z.; Kim, D. H.; Sargent, E. H. Perovskite energy funnels for efficient light-emitting diodes. *Nat. Nanotechnol.* **2016**, *11*, 872-877.

(12) Smith, I. C.; Hoke, E. T.; Solis-Ibarra, D.; McGehee, M. D.; Karunadasa, H. I. A layered hybrid perovskite solar-cell absorber with enhanced moisture stability. *Angew. Chem. Inter. Ed.* **2014**, *53*, 11232-11235.

(13) Byun, J.; Cho, H.; Wolf, C.; Jang, M.; Sadhanala, A.; Friend, R. H.; Yang, H.; Lee, T.-W. Efficient visible quasi-2D perovskite light-emitting diodes. *Adv. Mater.* **2016**, *28*, 7515-7520.

(14) Grancini, G.; Roldan-Carmona, C.; Zimmermann, I.; Mosconi, E.; Lee, X.; Martineau, D.;

Narbey, S.; Oswald, F.; De Angelis, F.; Graetzel, M.; Nazeeruddin, M. K. One-year stable perovskite solar cells by 2D/3D interface engineering. *Nat. Commun.* **2017**, *8*, 15684.

(15) Proppe. A. H.; Wei. M.; Chen. B.; Quintero-Bermudez. R.; Kelley. S. O.; Sargent. E. H. Photochemically cross-linked quantum well ligands for 2D/3D perovskite photovoltaics with improved photovoltage and stability. *J. Am. Chem. Soc.* **2019**, *141*, 14180-14189.

(16) Shi. D.; Adinolfi. V.; Comin. R.; Yuan. M.; Alarousu. E.; Buin. A.; Chen. Y.; Hoogland. S.; Rothenberger. A.; Katsiev. K.; Losovyj. Y.; Zhang. X.; Dowben. P. A.; Mohammed. O. F.; Sargent. E. H.; Bakr. O. M. Low trap-state density and long carrier diffusion in organolead trihalide perovskite single crystals. *Science* **2015**, *347*, 519-522.

(17) Stranks, S. D.; Eperon, G. E.; Grancini, G.; Menelaou, C.; Alcocer, M. J. P.; Leijtens, T.; Herz, L. M.; Petrozza, A.; Snaith, H. J. Electron-hole diffusion lengths exceeding 1 micrometer in an organometal trihalide perovskite absorber. *Science* **2013**, *342*, 341-344.

(18) Xing, G.; Mathews, N.; Sun, S.; Lim, S. S.; Lam, Y. M.; Graetzel, M.; Mhaisalkar, S.; Sum, T. C. Long-range balanced electron- and hole-transport lengths in organic-inorganic $CH_3NH_3PbI_3$. *Science* **2013**, *342*, 344-347.

(19) Dong. Q.; Fang. Y.; Shao. Y.; Mulligan. P.; Qiu. J.; Cao. L.; Huang. J. Electron-hole diffusion lengths >175 μm in solution-grown $CH_3NH_3PbI_3$ single crystals. *Science* **2015**, *347*, 967-970.

(20) Umansky, V.; de-Picciotto, R.; Heiblum, M. Extremely high-mobility two dimensional electron gas: Evaluation of scattering mechanisms. *Appl. Phys. Lett.* **1997**, *71*, 683-685.

(21) Zarem, H. A.; Sercel, P. C.; Lebens, J. A.; Eng, L. E.; Yariv, A.; Vahala, K. J. Direct determination of the ambipolar diffusion length in GaAs/AlGaAs heterostructures by

cathodoluminescence. *Appl. Phys. Lett.* **1989**, *55*, 1647-1649.

(22) Drummond, T. J.; Morkoç, H.; Hess, K.; Cho, A. Y. Experimental and theoretical electron mobility of modulation doped $Al_xGa_{1-x}As$/GaAs heterostructures grown by molecular beam epitaxy. *J. Appl. Phys.* **1981**, *52*, 5231-5234.

(23) Blancon, J. C.; Stier, A. V.; Tsai, H.; Nie, W.; Stoumpos, C. C.; Traore, B.; Pedesseau, L.; Kepenekian, M.; Katsutani, F.; Noe, G. T.; Kono, J.; Tretiak, S.; Crooker, S. A.; Katan, C.; Kanatzidis, M. G.; Crochet, J. J.; Even, J.; Mohite, A. D. Scaling law for excitons in 2D perovskite quantum wells. *Nat. Commun.* **2018**, *9*, 2254.

(24) Wu, X.; Trinh, M. T.; Zhu, X. Excitonic many-body interactions in two-dimensional lead iodide perovskite quantum wells. *J. Phys. Chem. C* **2015**, *119*, 14714-14721.

(25) Tanaka, K.; Kondo, T. Bandgap and exciton binding energies in lead-iodide-based natural quantum-well crystals. *Sci. Technol. Adv. Mater.* **2003**, *4*, 599-604.

(26) Blancon, J. C.; Tsai, H.; Nie, W.; Stoumpos, C. C.; Pedesseau, L.; Katan, C.; Kepenekian, M.; Soe, C. M. M.; Appavoo, K.; Sfeir, M. Y.; Tretiak, S.; Ajayan, P. M.; Kanatzidis, M. G.; Even, J.; Crochet, J. J.; Mohite, A. D. Extremely efficient internal exciton dissociation through edge states in layered 2D perovskites. *Science* **2017**, *355*, 1288-1291.

(27) Deng, S.; Shi, E.; Yuan, L.; Jin, L.; Dou, L.; Huang, L. Long-range exciton transport and slow annihilation in two-dimensional hybrid perovskites. *Nat. Commun.* **2020**, *11*, 664.

(28) Tian, W.; Zhao, C.; Leng, J.; Cui, R.; Jin, S. Visualizing carrier diffusion in individual single-crystal organolead halide perovskite nanowires and nanoplates. *J. Am. Chem. Soc.* **2015**, *137*, 12458-12461.

(29) Tian, W.; Leng, J.; Zhao, C.; Jin, S., Long-distance charge carrier funneling in perovskite

nanowires enabled by built-in halide gradient. *J. Am. Chem. Soc.* **2017**, *139*, 579-582.

(30) Tian. W.; Cui. R.; Leng. J.; Liu. J.; Li. Y.; Zhao. C.; Zhang. J.;Deng. W.; Lian. T.; Jin. S. Limiting perovskite solar cell performance by heterogeneous carrier extraction. *Angew. Chem. Int. Ed.* **2016**, *55*, 13067-13071.

(31) Shi, E.; Deng, S.; Yuan, B.; Gao, Y.; Akriti; Yuan, L.; Davis, C. S.; Zemlyanov, D.; Yu, Y.; Huang, L.; Dou, L. Extrinsic and dynamic edge states of two-dimensional lead halide perovskites. *ACS Nano* **2019**, *13*, 1635-1644.

(32) Zhao, C.; Tian, W.; Leng, J.; Zhao, Y.; Jin, S. Controlling the property of edges in layered 2D perovskite single crystals. *J. Phys. Chem. Lett.* **2019**, *10*, 3950-3954.

(33) Wang, K.; Wu, C.; Jiang, Y.; Yang, D.; Wang, K.; Priya, S. Distinct conducting layer edge states in two-dimensional (2D) halide perovskite. *Sci. Adv.* **2019**, *5*, 3241.

(34) Dou, L.; Wong, A. B.; Yu, Y.; Lai, M.; Kornienko, N.; Eaton, S. W.; Fu, A.; Bischak, C. G.; Ma, J.; Ding, T.; Ginsberg, N. S.; Wang, L.; Alivisatos, A. P.; Yang, P. Atomically thin two-dimensional organic-inorganic hybrid perovskites. *Science* **2015**, *349*, 1518-1521.

(35) Zhai, Y.; Baniya, S.; Zhang, C.; Li, J.; Haney, P.; Sheng, C.-X.; Ehrenfreund, E.; Vardeny, Z. V. Giant Rashba splitting in 2D organic-inorganic halide perovskites measured by transient spectroscopies. *Sci. Adv.* **2017**, *3*, 1700704.

(36) Motta, C.; El-Mellouhi, F.; Kais, S.; Tabet, N.; Alharbi, F.; Sanvito, S. Revealing the role of organic cations in hybrid halide perovskite $CH_3NH_3PbI_3$. *Nat. Commun.* **2015**, *6*, 7026.

(37) Azarhoosh, P.; McKechnie, S.; Frost, J. M.; Walsh, A.; van Schilfgaarde, M. Research Update: Relativistic origin of slow electron-hole recombination in hybrid halide perovskite solar cells. *APL Mater.* **2016**, *4*, 091501.

(38) Nirmal, M.; Norris, D. J.; Kuno, M.; Bawendi, M. G.; Efros, A. L.; Rosen, M., Observation of the "Dark exciton" in CdSe quantum dots. *Phys. Rev. Lett.* **1995**, *75*, 3728-3731.

(39) Utterback, J. K.; Grennell, A. N.; Wilker, M. B.; Pearce, O. M.; Eaves, J. D.; Dukovic, G. Observation of trapped-hole diffusion on the surfaces of CdS nanorods. *Nat. Chem.* **2016**, *8*, 1061-1066.

(40) Wu, K.; Du, Y.; Tang, H.; Chen, Z.; Lian, T., Efficient extraction of trapped holes from colloidal CdS nanorods. *J. Am. Chem. Soc.* **2015**, *137*, 10224-10230.

(41) Zhu, H.; Song, N.; Rodriguez-Cordoba, W.; Lian, T. Wave function engineering for efficient extraction of up to nineteen electrons from one CdSe/CdS quasi-type II quantum dot. *J. Am. Chem. Soc.* **2012**, *134*, 4250-4257.

(42) Wu, K.; Zhu, H.; Liu, Z.; Rodriguez-Cordoba, W.; Lian, T. Ultrafast charge separation and long-lived charge separated state in photocatalytic CdS-Pt nanorod heterostructures. *J. Am. Chem. Soc.* **2012**, *134*, 10337-10340.

(43) Leventis, H. C.; O'Mahony, F.; Akhtar, J.; Afzaal, M.; O'Brien, P.; Haque, S. A. Transient optical studies of interfacial charge transfer at nanostructured metal Oxide/PbS quantum dot/organic hole conductor heterojunctions. *J. Am. Chem. Soc.* **2010**, *132*, 2743-2750.

(44) Li, W.; Liu, J.; Bai, F. Q.; Zhang, H. X.; Prezhdo, O. V. Hole trapping by iodine interstitial defects decreases free carrier losses in perovskite solar cells: A time-domain Ab initio study. *ACS Energy Lett.* **2017**, *2*, 1270-1278.

(45) Delport, G.; Chehade, G.; Ledee, F.; Diab, H.; Milesi-Brault, C.; Trippe-Allard, G.; Even, J.; Lauret, J. S.; Deleporte, E.; Garrot, D. Exciton-exciton annihilation in two-dimensional halide perovskites at room temperature. *J. Phys. Chem. Lett.* **2019**, *10*, 5153-5159.

TOC

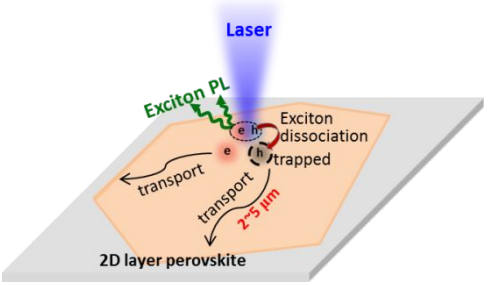
Laser
Exciton PL
Exciton
dissociation
trapped
transport
transport
2~5 μm
2D layer perovskite